Proceedings IRF2018: 6th International Conference Integrity-Reliability-Failure
Lisbon/Portugal 22-26 July 2018. Editors J.F. Silva Gomes and S.A. Meguid
Publ. INEGI/FEUP (2018); ISBN: 978-989-20-8313-1

PAPER REF: 7265

FAULT DETECTION IN DIESEL ENGINE INJECTORS USING A VIBRATION AND SOUND PRESSURE LEVEL TECHNIQUE

Jarbas Santos Medeiros(*), Daniel Mousinho Lago, Antônio Adalberto Cavalcante Moreira Filho, Efrain Pantaleon Matamoros, João Telésforo Nóbrega de Medeiros
Federal University of Rio Grande do Norte (UFRN), Natal-RN, Brazil
(*)*Email:* jarbas_inf@yahoo.com.br

ABSTRACT

This article presents a study on the time series of vibration signals and sound pressure level of a diesel engine injector, operating with different fuels, identifying signal processing parameters that correlate with the operation and wear regimes of the component. The tests were performed in a commercial test rig TM-507, using 3 fluids: B6 added with tensoactives; B6 with tensoactives and water; and B6 with tensoactives, water and glycerin in order to induce different wear mechanisms at the nozzle tip. The signal processing and analysis were performed using Matlab and time-frequency analysis through the wavelet transform and RMS of 6 frequency bands. The results were promising and showed that it is possible to correlate frequency bands of the signals with the different wear mechanisms of diesel engine injector (EI). Such tools proved to be valuable and can be integrated into a future generation of fuel injection or On Board Diagnosis systems to help with defects diagnose and minimize pollutant emissions.

Keywords: diesel engine, biodiesel, wear, common rail injector.

INTRODUCTION

Diesel vehicles are the most responsible sources of emission of fine PM particles, that cause respiratory diseases, and also for the NOx production. The fuel injection and management system of those vehicles, Common Rail, aims to control the amount of diesel injected into the combustion chamber in order to obtain the complete combustion of the fuel and to mitigate the emission of polluting particles and gases. The diesel EI is the component responsible for the atomization of the fuel in the combustion chamber and its integrity is of great importance in the proper functioning of the engine as well as in the maintenance of the emission levels of polluting gases within the recommended limits. The EI works in transient regimes, severe conditions of temperature, pressure, and it is subjected to erosion, cavitation, adhesion and corrosion mechanisms, making it difficult to predict or prevent possible failures (Oliveira, 2016).

Chagas da Silva (2015), performed an interview with seven experienced mechanics about the occurrence of injector nozzle failures in which a consensus was noticed about there is no how predict when an EI is going to fail, due to variables related to the failure. In the interviews, it was reported that some diesel EI presented failures within 10,000 kilometers while other engines ran 400,000 before the first failure. However, the manufacturers recommend repairs and bench tests to visualize spraying in the EI at each 100,000 kilometers. The mechanics also

reported that the main causes for the failures are the lack of preventive maintenance and the quality of the fuel.

Osipowicz and Kowalek (2014) evaluated the performance of some EI and identified through microscopy severe damages to the components, however the damaged nozzles preserved their performance when analyzed under the light of flow rate and leak testing which are criterias recommended by the manufacturer.

Due to such problems, many studies aim to identify failures in EI using different monitoring and data analysis techniques.

Moshou *et al*. (2014), used One-Class Support Vector Machine (OCSVM) and One-Class Self Organizing Map (OCSOM) techniques to detect failures in diesel injector nozzles, acquiring sound pressure level and using signal treatment techniques, with the usage of a microphone in agricultural diesel engines. Their results show that those methods have been found to be efficient and adaptive for detecting automatic failures in agricultural tractor engines.

Ftoutou and Chouchane (2017), used time-frequency and angle-frequency analysis in vibration signals through STFT to identify failures in the fuel injection in diesel engines.

The present study aims to evaluate the predictive maintenance, vibration and sound pressure level techniques to diagnose operation failures of a diesel injector nozzle in a test rig under different wear mechanisms, induced by 3 different fuels.

MATERIALS AND METHODS

The atomization and wear tests were performed in a commercial rig, called Diesel Injector Test - TM-507, manufactured by the company Tecnomotor located in the city of São Carlos, Brazil, Figure 1. The evaluated nozzles were new Common Rail piezoelectrics type, manufactured by Bosch do Brasil, with reference code DLLA 148 P1067.

Fig. 1 - Test rig Diesel Injector Test TM 507 Common Rail

The test rig had a standard configuration in which the nozzles were evaluated in four simulated engine operating regimes: pre-injection, low load, partial load and full load. These tests had a fixed and limited time window, just a few seconds, making it impossible to carry out the long duration tests. In this way, it was necessary the collaboration of the manufacturer,

TECNOMOTOR, to create new software that would allow to set the test time to last longer. After this software update, the machine had its maximum operating time modified to approximately 3 hours and 45 minutes, thus allowing the tests to be performed in stages. The partial load parameters were selected: injection time of 700 μs, frequency of 18 Hz (2160 rpm) and pressure of 800 bar. The tests were performed individually and the atomization was performed in a cylindrical glass chamber with atmospheric pressure and ambient temperature.

The microemulsions were prepared using S10 mineral diesel (10 ppm sulfur and 6% biodiesel), the so-called R4 and R6 surfactants and the aqueous glycerin solution, which according to the informations given by the manufacturer of the products, ULTRANEX NP 40 and ULTRANEX NP 60, it is a mixture of chemical nature of alkyl-phenyl glycolic polyethers. The formulation was obtained by adding 1.75% (blending volume) of surfactant R4 + 1.75% (blending volume) of surfactant R6 + 4.0 ml of distilled water for each 100 ml of pure diesel. The emulsion was maintained under mechanical stirring and the aqueous solution of glycerin was then added until it reached the turbidity point.

The lubricity of a lubricant is its ability to minimize friction and wear between the surfaces in contact under load and relative movement between them. In this study, the fluid lubricity was evaluated through tests on the High Frequency Reciprocating Rig bench (HFRR), from PCS Instruments, Figure 2, available at the Laboratory of Tribology and Structural Integrity of UFRN. The HFRR test is a lubricated tribological test in which an alternating movement of a sphere on a plane (both AISI 52100 steel) is performed according to the conditions established by ASTM D6079 (2016), which are described in Table 1. The lubricity is evaluated, considering the mean wear scar diameter generated on the sphere, due to its relative movement with de plane.

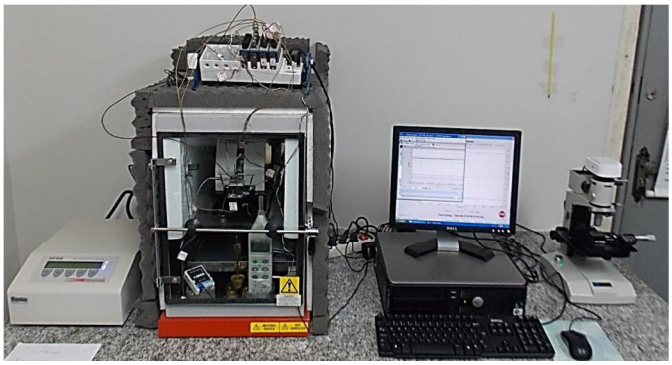

Fig. 2 - HFRR test rig

Table 1 - HFRR test parameters

Parameter:	**Condition:**
Material	52100 steel (disc and sphere)
Load	2 N
Temperature	60 °C
Time	75 minutes
Frequency	50 Hz

The signals acquisition was performed using software developed in the LabView® graphic programming language. The system used was the CompactDaq with the NI 9205 module for volume reading, 24-bit resolution, and the NI 9234 module with 12-bit resolution for editing

the analog output of the decibel meter, Figure 3. It was used a sampling rate of 50 KHz and a sampling time of 0.24 seconds. The accelerometer was positioned in the direction of actuation of the injection needle of the injector nozzle.

Fig. 3 - Sound level meter and signals acquisition modules

The NPS and vibration signal analysis was performed from the time evolution of the sample rms measured in 10 second windows. Each point of the RMS graphs was calculated from each sample which has 12,000 points. The frequency domain analysis of the signals was performed through the continuous wavelet transform that is calculated by the convolution of the signal of each sample with a wavelet function according to the following equation:

$$CWT_f(a,b) = \frac{1}{\sqrt{a}} \int_{-\infty}^{\infty} f(t) \cdot \psi^* \left(\frac{t-b}{a} \right) dt, \qquad (1)$$

Where a is the scale parameter, b is the translation parameter, $f(t)$ is the signal in time domain, ψ is the mother wavelet and ψ^* is the complex conjugated of ψ.

onde a é o parâmetro escala, b é o parâmetro translação, $f(t)$ é o sinal do domínio do tempo, ψ é wavelet mãe, e ψ^* é o conjugado complexo de ψ.

The continuous wavelet transform (CWT) generates a two-dimensional map of coefficients called scalogram, according to the following equation:

$$SC\{f(a,b)\} = \left| CWT_f(a,b) \right|^2 =$$
$$= \left| \int_{-\infty}^{\infty} f(t) \cdot \frac{1}{\sqrt{a}} \psi^* \left(\frac{t-b}{a} \right) dt \right|^2. \qquad (2)$$

It is defined as the square magnitude of the CWT, and has the scale converted to frequency from the center frequency of the mother wavelet, used in the analysis. The mother wavelet function used to analyze the signals in this study was the Morlet one.

RESULTS

The fuel lubricity analysis made by the HFRR, showed that the B6 + surfactant fuel achieves the worst Wear Scar Diameter (WSD) result of 310 µm, Figure 4(a), followed by B6 + surfactants + water with a WSD of 298 µm, Figure 4(b). The best result was obtained with the fuel B6 + surfactants + water + glycerin that obtained WSD equal to 166 µm. Figure 4(c) shows the generated scars on the spheres during the HFRR tests with the fuels under analysis.

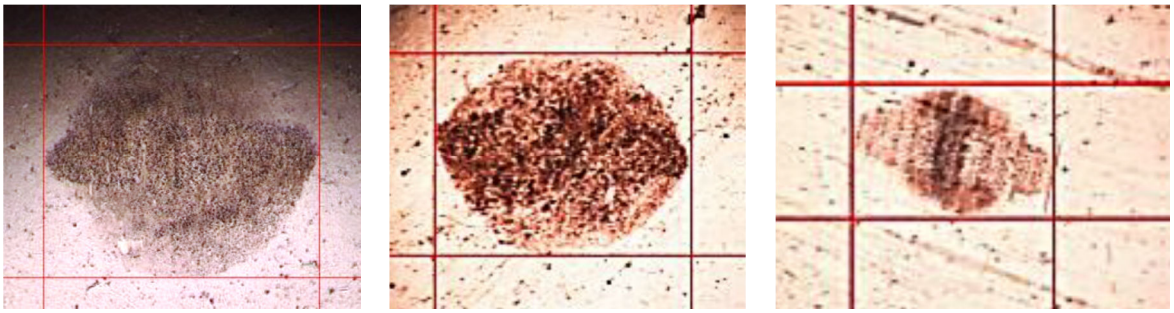

(a) WSD 310 µm (b) WDS 298 µm (c) WSD 166 µm

Fig. 4 - HFRR WSD measurements

The SEM analysis allowed to identify different wear mechanisms that acted on the nozzles. Figure 5 shows the internal image of the injector in the new condition.

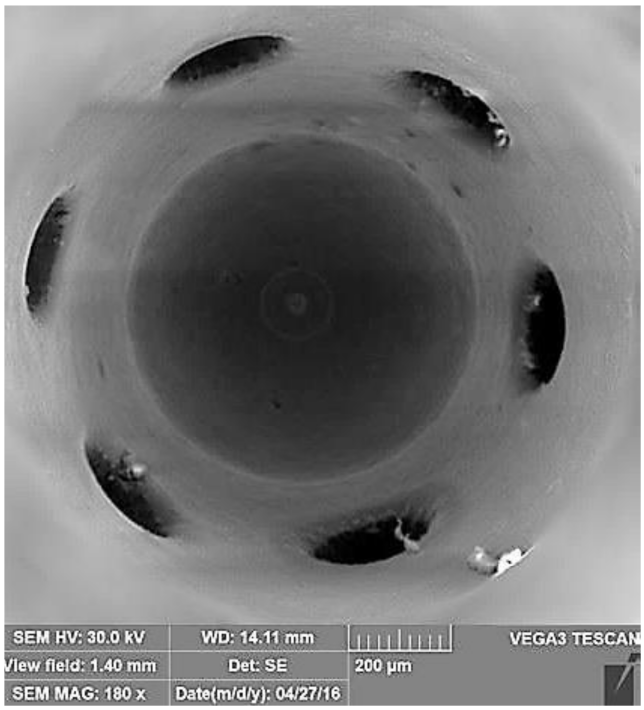

Fig. 5 - SEM (SE) image of the interior of the injector nozzle

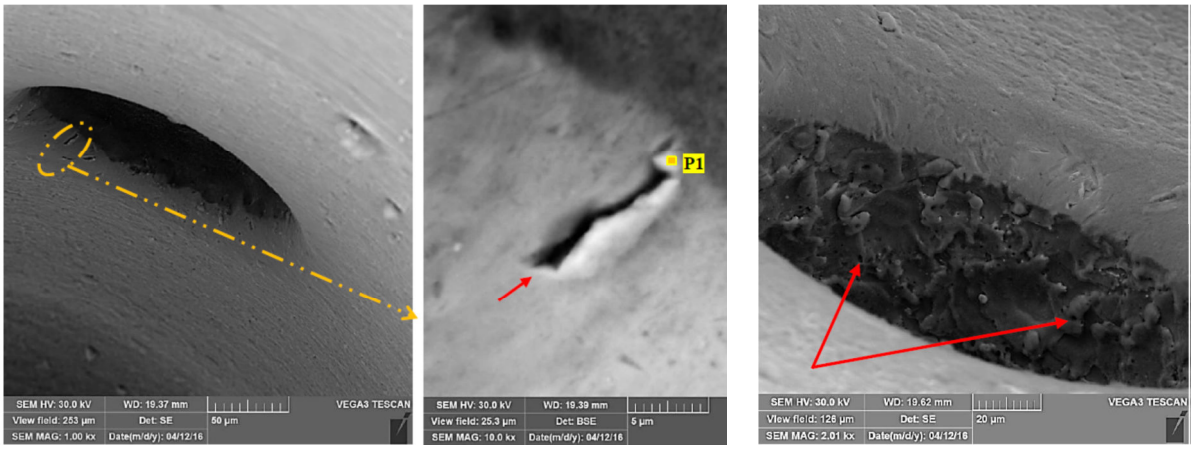

(a) (b) (c)

Fig. 6 - Inner surface of the injector nozzle

The images of Figure 6 correspond to the inner surface of the nozzle, located at 1h position. Figure 6(b) shows evidence of abrasive wear on the lower edge of the nozzle with scratches or grooves. The grooves formed in this region probably arise due to the displacement of a hard particle in the substrate of the nozzle's wall.

In most of the surfaces of these nozzles, there was found micropithe formation downstream of the nozzle entrance edge, Figure 6(c). They are the result of the synergism between erosion and cavitation and they have a diameter of approximately 2µm.

Figure 7, obtained by SEM (SE and BSE), exhibit the surfaces of the nozzles of a Common Rail injector after 20 hours of non-continuous atomization tests with B6 + tensoactives + water.

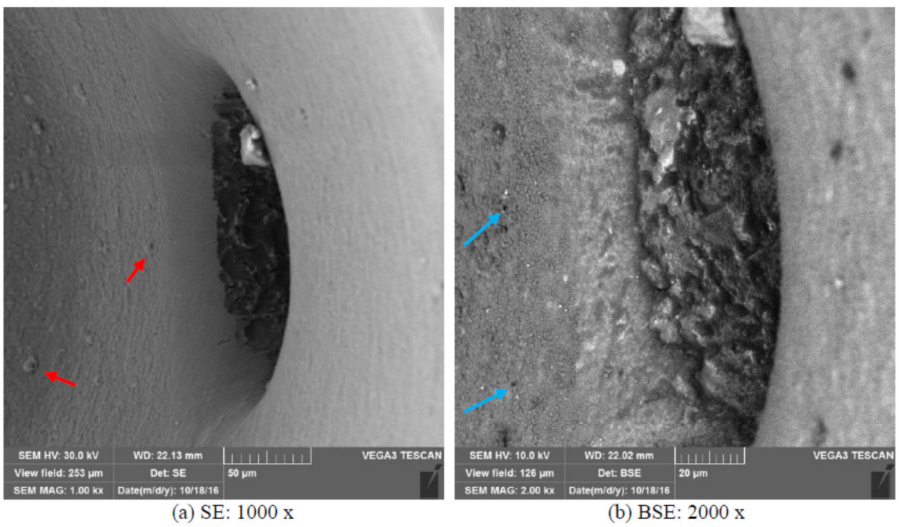

(a) SE: 1000 x (b) BSE: 2000 x

Fig. 7 - SEM images of the inner surface of the nozzle at position 3h showing (a) particle at the upper edge of the nozzle, micro-spalling (red arrows) simultaneously with erosive wear on the left wall texture and (b) micropites, indicated by arrows.

The inner surfaces of the nozzle at position 3h, Figure 7, obtained by SEM, in which it is observed (a) micro-spalling, erosive wear, more evident by the wall texture at the left of the nozzle, and (b) micropits at the periphery of the nozzle.

Figure 8, obtained by SEM (SE and BSE), shows the surfaces of the nozzles of a Common Rail injector after 62 hours of non-continuous atomization tests, using B6 + tensoactives + water + glycerine fuel.

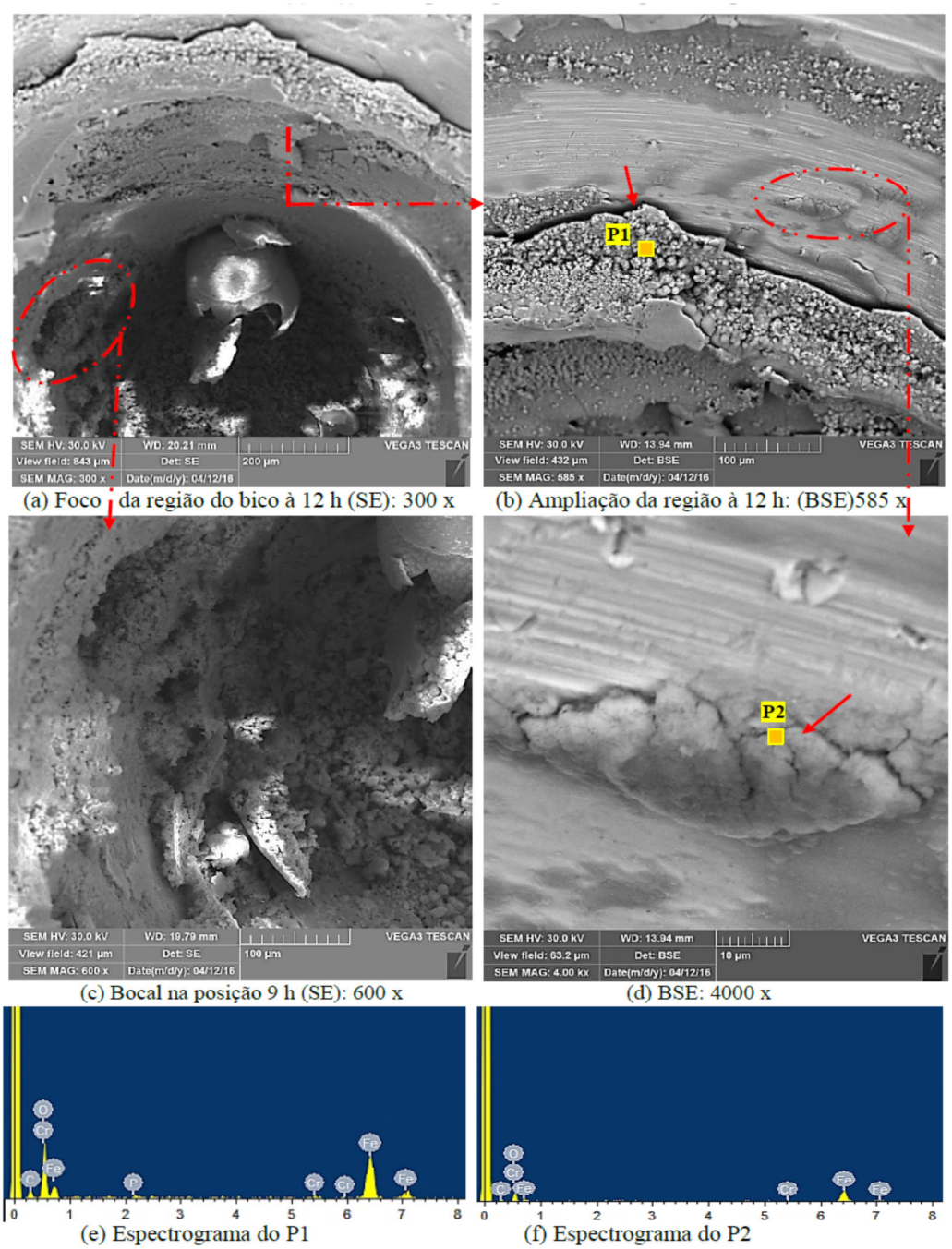

Fig. 8 - SEM images of the upper inner surface of the nozzle. In (a) nozzle obstruction at 11 h. In (b) shows the britle fracture in the oxidized layer, whose magnification in (d) allows to observe microcracks. In (c) magnification of the nozzle at position 9 h.

Figure 8 shows: (a) evidence of severe erosive and oxidative wear mechanisms, detailed in (b) and (c). In (b) the upper surface region at the 12 h position is shown, evidencing the brittle fracture of an oxidized layer. In (d), the presence of microcracks of oxidized layers that are in

an expansion process, in the imminence of detachment. The points P1 (C, O, Fe, Cr, and P) and P2 (C, O, Fe, Cr) indicated in the oxide layers of Figure 6 were identified by EDS in the spectrograms shown in (e) and (f), respectively.

In the following topics, they are presented the time series of the vibration and NPS signals, obtained in the different tests. The RMS time series of the vibration of the three tests is shown in the Figure 9 below. It was noticed that the injector nozzle which worked with glycerin in the fuel formulation, when it reached the 15 hour of testing, it presented a sudden change in the signal level by doubling its intensity, reaching the highest value of all 3 tests, 8 gms. This change is possibly related to the transition from the oxidative to severe oxidative wear mechanism in which the oxide layer reached a thickness limit and began to crack as observed in SEM images. After identifying this transition, assuring the severity of the damage, the test was reprogrammed until it reached the catastrophic failure of the diesel injector nozzle that occurred at 62 hours of test when it completely stopped working.

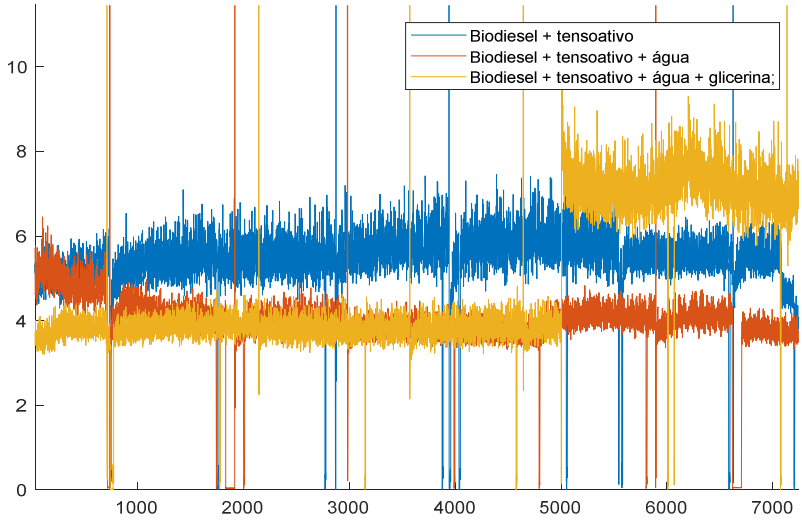

Fig. 9 - Vibration signal of the injector nozzle, working with the 3 tested fuels.

It is also observed in Figure 9 that the vibration signal of the EI which worked with B6 + tensoactives was kept almost constant and reached the same level as observed when the oxidative wear mechanism occurred in the test performed with the glycerol in fuel composition. Probably, the water present in the fuel formulation contributed to the formation of a thin oxide layer which during the 20 hours of testing contributed to the reduction of the friction, reducing the vibration of the engine injector. Although the SEM images showed the erosive-cavitative and micro-spalling wear mechanisms. It is very likely that oxidation is the predominant wear mechanism for this test.

The injector which worked without water in the fuel composition had the highest vibration levels during the 15 hours of the test while the other injectors possibly presented the predominance of oxidative wear mechanism in that period.

The time series of NPS signal, Figure 10, shows that the response of the EI with predominance of erosive-cavitative wear was increasing, with the maximum level of 45 mV

(B6 + tensoactive). The signal obtained using B6 + tensoactives showed to be decreasing, reaching the level of 35 mV at the end of the test, which is the same level as the test in which severe oxidative wear occurred. The injector nozzle that ran with glycerin in the fuel, presented the lower NPS level compared to the other tested injectors. However, the NPS signal was unable to detect the transition from regular oxidative wear to severe oxidative wear as identified by the vibration signal. These data showed a direct correlation between NPS signal and lubricity of the fuel, quantified by the WSD in HFFR tests, which is related to the biodiesel content.

The time series of SPL, Figure 10, show that the response of the EI with predominance of erosion-cavitation wear was increasing reaching the maximum value of 45 mV (B6 + tensoactive). The EI signal using B6 + surfactant + water decreased, ending the test at 35 mV, at the same level as the test that presented severe oxidative wear. The injector nozzle that used the glycerin in the fuel obtained the lowest SPL in relation to the other tests, however the SPL could not detect the transition from the oxidative mechanism to severe oxidative, as was possible with the vibration signal. These data showed that the SPL presented a direct correlation with the WSD quantified in the HFFR test that, according to Farias (2013), is related to the biodiesel content, however the SPL was not sensitive to the oxidative wear mechanism of the diesel injector nozzle.

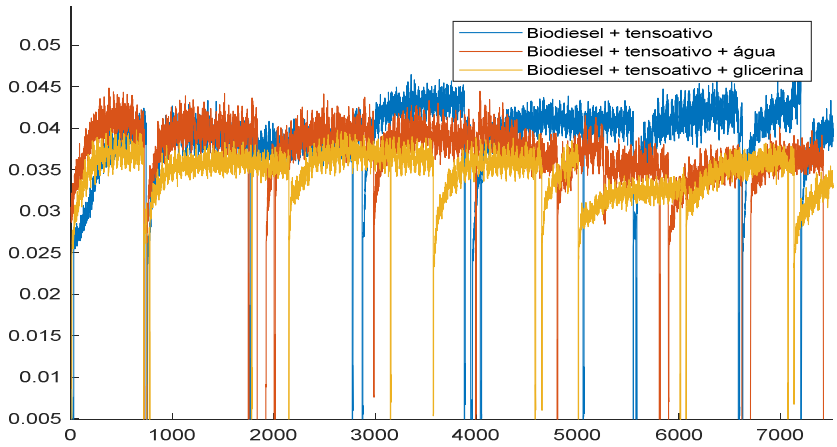

Fig. 10 - NPS signal emitted by the injector nozzle, when working with the 3 tested fuels.

In order to better understand the effects of the wear mechanisms on the studied signals, a time-frequency analysis was performed by means of the wavelet transform in which it was sought to identify which frequencies are related to the wear mechanisms identified in the diesel injector nozzles. The frequency spectrum was divided into the following bands: FB1 (0 - 781 Hz), FB2 (781 - 1560 Hz), FB3 (1560 - 3120 Hz), FB4 (3120 - 6250 Hz), FB5 (6250 - 12500 Hz), e FB6 (12500 - 25000 Hz).

The following Figure 11. shows the vibration signal spectrogram of a sample from each test as well as the RMS of the six frequency bands. (A) and (b) are from the B6 + tensoactive test, (c) and (d) from B6 + tensoactive + water test, (e) and (f) are from the test that run with B6 + water + glycerin. The samples were obtained after approximately 19 h of test when the predominant mechanisms of erosive-cavitative, oxidative and oxidative wear were observed in each test.

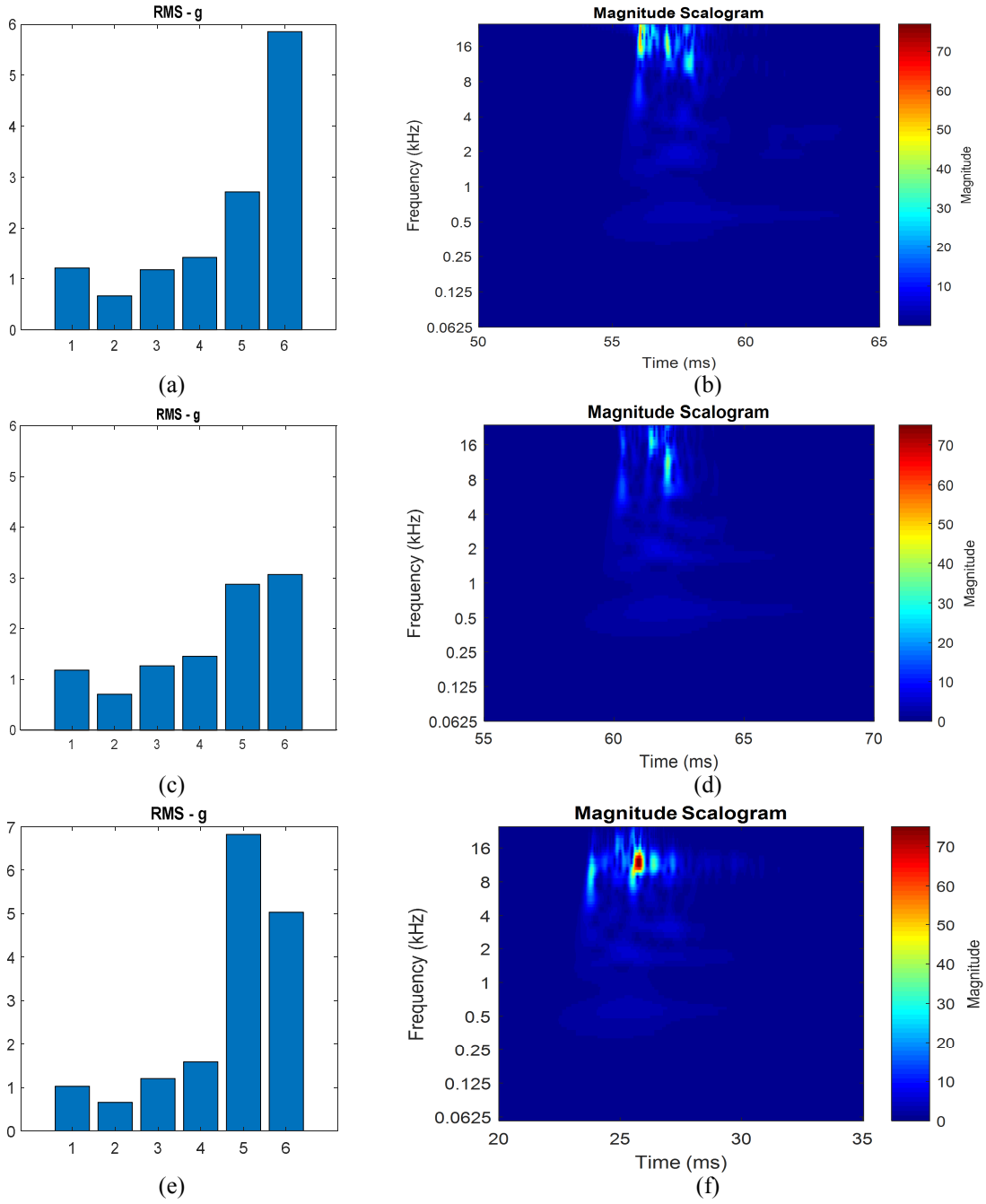

Fig. 11 - Vibration signal spectrogram of a sample from each test and the RMS of the six frequency bands. In (a) and (b) are from the B6 + tensoactive test, (c) and (d) from B6 + tensoactive + water test, (e) and (f) are from the test that run with B6 + water + glycerin.

It is observed in the bar graph, Figure 11(a), that when the predominant mechanism is cavitation-erosion the FB6 frequency band has the highest energy in the vibration signal. The spectrogram of this signal showed that this higher energy occurs during the beginning of fuel injection. When the wear mechanism is predominantly oxidative, Figure 11(c), the energies of the frequency bands FB5 and FB6 are approximately equal, but when the predominant mechanism is the severe oxidative, Figure 11(e), FB5 has the highest energy. In this case the highest energy occurs at the final moments of the fuel injection according to the spectrogram in Figure 11(f).

The following Figure 12 shows the SPL signal spectrogram of a sample from each test as well as the RMS of the six frequency bands. (A) and (b) are from the B6 + tensoactive test, (c) and (d) from B6 + tensoactive + water test, (e) and (f) are from the test that run with B6 + water + glycerin. The samples were obtained at the same instants as the vibration samples that were analyzed.

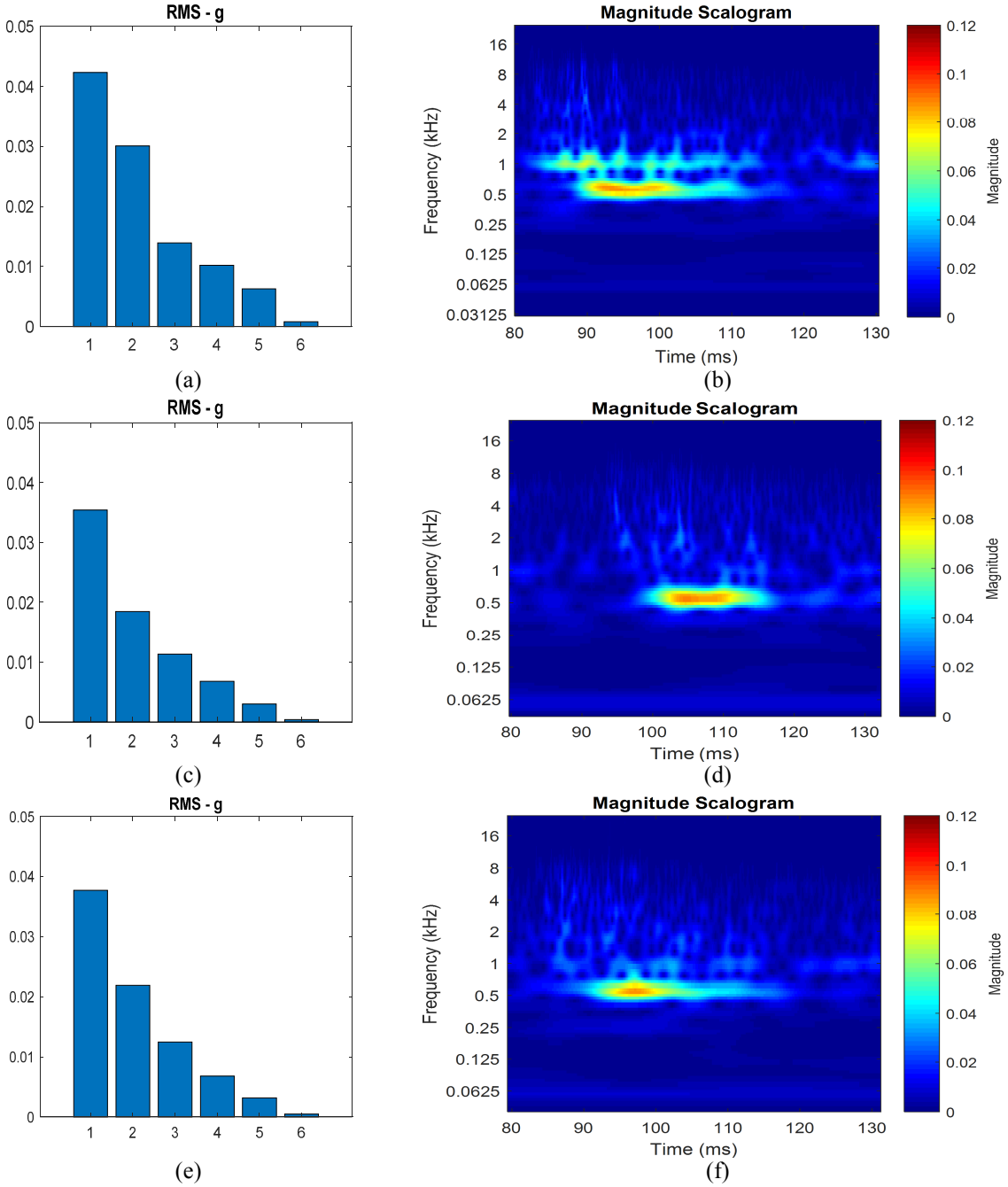

Fig.12 SPL signal spectrogram of a sample from each and the RMS of the six frequency bands. (a) and (b) are from the B6 + tensoactive test, (c) and (d) from B6 + tensoactive + water test, (e) and (f) are from the test that run with B6 + water + glycerin.

It is observed in Figure 12 that the frequency bands energy of the SPL samples of the three tests showed the same inverse behavior with respect to the frequencies. It should be noted that band B2 in (b), which is relative to the B6 + tensoactives test, has the highest energy in

relation to B2 from other tests and that the spectrogram (b) shows significant energy points with a frequency of 1 KHz. Such characteristics are possibly related to cavitation-erosion. The other graphs and spectrograms of the other two tests showed no significant differences and the SPL was not sensitive to the change from the oxidative mechanism to severe oxidative wear.

CONCLUSION

In this study it was observed that the vibration and sound pressure level, as predictive maintenance techniques, showed different characteristics in identifying damage to common rail injector nozzles when subjected to bench test. The SPL acquired from the nozzles tested with fuels of different lubricities showed a direct correlation with the WSD from the HFRR tests but did not corroborate with the damage severity generated in the injector nozzles. The RMS of the vibration signal measured in the needle motion direction was able to identify the transition from the oxidative to severe oxidative wear mechanism. The time-frequency analysis through the wavelet transform showed that the moment of greatest energy occurred in the beginning of fuel injection for the erosive-cavitative mechanisms and during the final moment for the severe oxidative. The peaks of energy of these signals also occur in different frequency bands.

The results are promising and showed that it is possible to correlate frequency bands of the vibration signals with the different wear mechanisms of diesel EI. Such tools proved to be valuable and can be integrated into a future generation of fuel injection or On-Board Diagnosis systems to help with defects diagnose and minimize pollutant emissions.

ACKNOWLEDGMENTS

The authors gratefully acknowledge the UFRN, Brazil, for experimental support, with a special mention to the laboratory of Tribology and Tecnomotor.

REFERENCES

[1] Osipowicz, T., Abramek, K.F., Stoeck, T. Testing of modern common rail fuel injectors. Combustion Engines.2015, 162(3), pp. 688-694.

[2] Mendes de Farias, Aline Cristina; Lubricidade de biodiesel e sua associação com a vibração e nivel de pressão sonara oriundos do contato esfera-plano sob deslizamento alternado, 2013

[3] Silva, Leonardo Chagas; Avaliação do desgaste triboquimico de agulhas dos bicos injetores em motores diesel operando com biodiesel, 2015.

[4] Ftoutou, Ezzeddine and Chouchane, Mnaouar; Injection Fault Detection of a Diesel Engine by Vibration Analysis, 2017.

[5] Moshou, Dimitrios *et al.* Fault Detection of Fuel Injectors Based on One-Class Classifiers. Modern Mechanical Engineering, v. 4, n. 1, pp. 19-27, 2014. Available from: <http://www.scirp.org/journal/doi.aspx?DOI=10.4236/mme.2014.41003>.